

Beyond Fixed Rounds: Data-Free Early Stopping for Practical Federated Learning

Youngjoon Lee¹, Hyukjoon Lee², Seungrok Jung², Andy Luo²,
 Jinu Gong³, Yang Cao⁴, and Joonhyuk Kang^{1†}

¹ School of Electrical Engineering, KAIST, South Korea

² AI Group, Advanced Micro Devices, Inc., United States

³ Department of Applied AI, Hansung University, South Korea

⁴ Department of Computer Science, Institute of Science Tokyo, Japan

yjlee22@kaist.ac.kr, jkang@kaist.ac.kr

Abstract. Federated Learning (FL) facilitates decentralized collaborative learning without transmitting raw data. However, reliance on fixed global rounds or validation data for hyperparameter tuning hinders practical deployment by incurring high computational costs and privacy risks. To address this, we propose a data-free early stopping framework that determines the optimal stopping point by monitoring the task vector’s growth rate using solely server-side parameters. The numerical results on skin lesion/blood cell classification demonstrate that our approach is comparable to validation-based early stopping across various state-of-the-art FL methods. In particular, the proposed framework spends an average of 47/20 (skin lesion/blood cell) rounds to achieve over 12.5%/10.3% higher performance than early stopping based on validation data. To the best of our knowledge, this is the first work to propose an early stopping framework for FL methods without using any validation data.

Keywords: Federated Learning· Task Vector· Early Stopping.

1 Introduction

Deep learning has driven significant advancements in medical imaging, utilizing large-scale datasets to achieve remarkable diagnostic performance [31]. However, the deployment of AI is strictly limited by stringent privacy regulations that prohibit the centralization of sensitive patient data [25,27]. To overcome this barrier, Federated Learning (FL) has emerged as a promising decentralized paradigm that facilitates collaborative learning without transmitting raw data [23]. By ensuring that data remain localized at their source, FL preserves data sovereignty and strictly adheres to institutional governance and ethical standards [20]. Moreover, FL enables robust and generalizable learning in medical AI by effectively leveraging cross-institutional data diversity [3]. Thus, FL provides a scalable and privacy-preserving solution well suited for the secure development of collaborative medical AI systems [10].

† Corresponding author

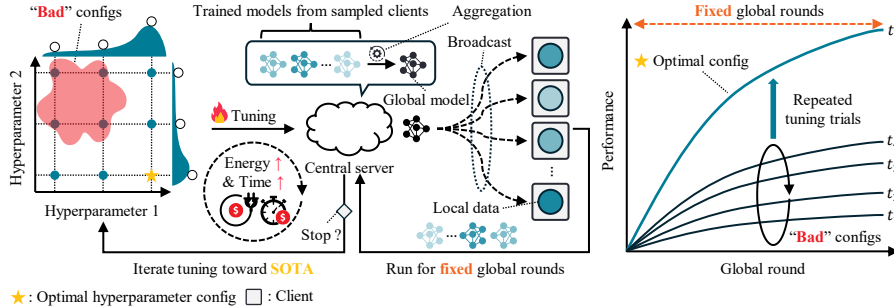


Fig. 1. Illustration of resource inefficiency in FL hyperparameter tuning. Since standard protocols use a fixed number of global rounds, ‘bad’ configurations waste computational and communication resources.

Recent FL methods have evolved to enhance convergence stability and performance by refining optimization strategies at the client or server level [4]. The foundational approaches are typically grounded in Stochastic Gradient Descent (SGD), where FL methods like FedAvg, FedProx [21], SCAFFOLD [12], and FedDyn [1] regulate updates to stabilize the learning process. Subsequently, advanced FL methods have shifted towards Sharpness-Aware Minimization (SAM) [8], which seeks flat minima rather than merely minimizing loss values. This paradigm has led to the development of SAM-based FL methods—including FedSAM [26], FedSpeed [29], FedSMOO [28], FedGamma [6], FedLESAM [7], and FedWMSAM [22]—that smooth and stabilize the optimization trajectory.

Despite the demonstrated effectiveness of recent FL methods, a practical constraint remains in their reliance on a pre-defined number of global rounds for training [14], as illustrated in Fig. 1. Similar to centralized learning, achieving optimal performance in FL requires extensive tuning of hyperparameters unique to each FL method or standard settings such as client-side learning rates [16]. In practice, this tuning process inevitably involves running ‘bad’ configurations that fail to converge to a satisfactory solution [13]. Under fixed-round protocols of FL, these ineffective configurations can cause high computational and communication overhead [18].

In this work, we propose a novel data-free early stopping framework that determines when to stop training using only the global model parameters at the server. Note that, unlike existing approaches relying on validation signals [15,24], our framework adopts a purely model-driven stopping criterion. By avoiding the need for validation data, our framework strictly adheres to the FL paradigm of model-only transmission [11]. We show that our approach seamlessly integrates with 10 state-of-the-art FL methods and remains robust across medical imaging datasets. Moreover, our framework maintains consistent stability under various non-IID distributions, effectively handling data heterogeneity. The extensive experiments validate that our strategy achieves generalization performance comparable to that of approaches relying on real validation data [33,35].

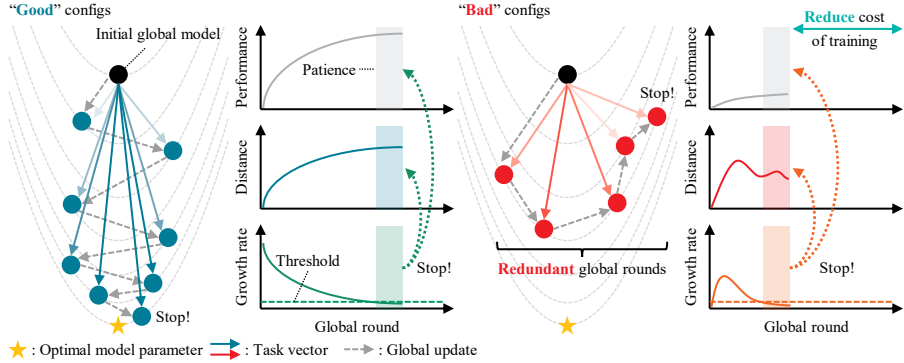


Fig. 2. Illustration of the proposed data-free early stopping framework. The server monitors the growth rate of the task vector using only global model parameters and stops training once the growth rate falls below the threshold. Here, the color intensity of the task vector reflects its increasing magnitude, and vice versa.

2 Problem and Method

2.1 Federated Setting

We consider a federated network comprising a central server and N clients, designed for medical image classification tasks. The system aims to optimize the global model parameters θ by minimizing the global objective function $F(\theta) \triangleq \frac{1}{N} \sum_{n=1}^N F_n(\theta)$, where $F_n(\theta)$ denotes the local objective function calculated over the private dataset of the n -th client. In each global round, a subset of M clients is randomly sampled to perform local learning. To simulate the non-IID nature, we consider three non-IID partitioning types following [19]: *Label skew* (Dirichlet, Pathological) and *Quantity skew*. For all considered distributions, the specific data allocation across clients is determined by a coefficient c .

2.2 Proposed Framework: Data-Free Early Stopping

We propose a novel early stopping framework that links federated convergence dynamics [5] with task vector characteristics [17] using only server-side global parameters, without relying on validation data. In detail, the FL process starts at global round $r = 1$ with an initialized model θ_0 . At each round $r \geq 1$, the central server aggregates M client-side local updates to obtain the global model θ_r through server-side optimization. We define the *global task vector* $\mathbf{v}_r \in \mathbb{R}^d$ as the cumulative displacement from the initialization:

$$\mathbf{v}_r := \theta_r - \theta_0 = \sum_{k=1}^r (\theta_k - \theta_{k-1}). \quad (1)$$

As training progresses, the global model moves away from the initialization, inducing an increasing task-specific displacement in the parameter space [9].

Algorithm 1 Proposed Data-Free Early Stopping

| | |
|---|---|
| 1: for $r = 1$ to R do | 11: CHECKEARLYSTOP (θ_r, r): |
| 2: for all selected clients in parallel do | 12: \triangleright Stopping criterion |
| 3: $\theta_r^m \leftarrow \text{CLIENTOPT}(\theta_{r-1})$ | 13: Compute \mathbf{v}_r using Eq. (1) |
| 4: end for | 14: if $r \geq 2$ then |
| 5: $\theta_r \leftarrow \text{SERVEROPT}(\{\theta_r^m\})$ | 15: Compute g_r using Eq. (3) |
| 6: $r^* \leftarrow \text{CHECKEARLYSTOP}(\theta_r, r)$ | 16: Update κ_r using Eq. (4) |
| 7: if $r^* > 0$ then return θ_{r^*} | 17: if $\kappa_r \geq \rho$ then return r |
| 8: end if | 18: end if |
| 9: end for | 19: end if |
| 10: return θ_R | 20: return 0 |

From an optimization perspective, each global update can be interpreted as a fine-tuning step resulting from the coupled dynamics of $\text{CLIENTOPT}(\cdot)$ and $\text{SERVEROPT}(\cdot)$. Under standard smoothness assumptions, the task vector approximates the accumulated gradient flow as:

$$\mathbf{v}_r \approx - \sum_{k=1}^r \gamma_k \nabla F(\theta_{k-1}). \quad (2)$$

Here, γ_r represents the effective step size determined by the local learning rate, the number of local steps, and the aggregation scaling. Since FL satisfies stationarity conditions, i.e., $\lim_{r \rightarrow \infty} \|\nabla F(\theta_r)\|_2 = 0$, the growth of \mathbf{v}_r diminishes as training converges. Thus, the accumulated optimization distance, $\delta_r := \|\mathbf{v}_r\|_2$, gradually converges to a stable value.

To capture this convergence behavior, we introduce the growth rate g_r , which quantifies the relative increase of the accumulated distance:

$$g_r = \frac{\delta_r - \delta_{r-1}}{\delta_{r-1}}, \quad r \geq 2. \quad (3)$$

As the learning trajectory stabilizes, g_r tends to decrease, indicating that later global updates contribute marginally to the overall displacement. This behavior reflects the onset of convergence in the parameter space. To be consistent with data-based early stopping, the proposed criterion is restricted to two hyperparameters: a sensitivity threshold τ and a patience parameter ρ . In particular, we define a recursive saturation counter κ_r as:

$$\kappa_r = \mathbb{I}(g_r < \tau) \cdot (\kappa_{r-1} + 1), \quad \kappa_1 = 0, \quad (4)$$

where $\mathbb{I}(\cdot)$ denotes the indicator function. The federated training process is stopped at the round r^* satisfying:

$$r^* = \min\{r \geq 2 \mid \kappa_r \geq \rho\}. \quad (5)$$

The overall framework and procedure are shown in Fig. 2 and Algorithm 1.

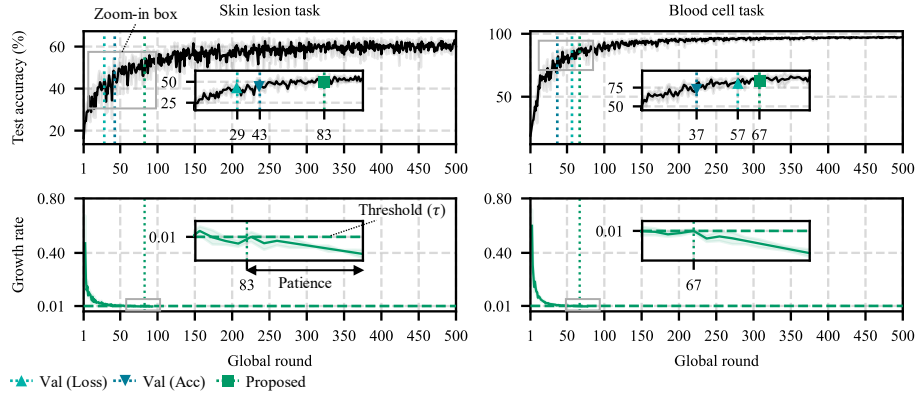


Fig. 3. Test accuracy (%) and growth rate trajectories over global rounds with $\tau = 0.01$ and $\rho = 10$ for both proposed and validation-based early stopping. The zoom-in boxes highlight the regions around the early stopping points.

3 Experiment and Results

3.1 Experiment Setting

We evaluate the proposed approach against validation-based early stopping using validation loss or accuracy on skin lesion [30] and blood cell [2] image classification tasks. Note that the baselines use both training and validation splits in [34], while our approach uses only the training subset. All clients employ ConvNeXtV2 [32] as the local AI model. We benchmark with recent FL methods, including FedAvg, FedProx, SCAFFOLD, FedDyn, FedSAM, FedSpeed, FedSMOO, FedGamma, FedLESAM, and FedWMSAM. To simulate the federated setting, the dataset is partitioned across $N = 100$ clients, and a subset of $M = 10$ clients is randomly sampled for local training at each round. The experiments are repeated with 3 random seeds, and our code is available at this repository.

3.2 Numerical Results

Effectiveness of Proposed Framework To show the effectiveness of the proposed framework, as shown in Fig. 3, we evaluate FedAvg under *label skew* (Dirichlet) with $c = 0.1$ and compare it against validation-based early stopping. On the skin lesion task, our approach stops, on average, +47 rounds later than validation-based early stopping, while achieving more than +12.5% higher performance. For the blood cell task, it extends training by about +20 rounds, while consistently improving performance, with a mean gain of +10.3%. Moreover, the lower panels of Fig. 3 show that the proposed growth rate metric gradually decays over rounds, leading to stable stopping at the predefined threshold. Overall, the results indicate that the proposed early stopping framework achieves validation-level performance without requiring any validation data.

Table 1. Performance comparison under diverse non-IID data distributions and coefficient values c with $\tau = 0.01$ and $\rho = 10$. Each value denotes the mean test accuracy difference between the proposed stopping point and the best-performing validation-based stopping point. The positive and negative values are highlighted in blue and red, respectively, where color intensity reflects the absolute magnitude of the difference. Note that bold and underlined values indicate the largest value for each c .

| Method | Label skew (Dirichlet) | | | Label skew (Pathological) | | | Quantity skew | | |
|------------------|------------------------|---------------|---------------|---------------------------|---------------|---------------|---------------|---------------|--------------|
| | $c = 0.01$ | $c = 0.1$ | $c = 1.0$ | $c = 1$ | $c = 2$ | $c = 3$ | $c = 0.01$ | $c = 0.1$ | $c = 1.0$ |
| Skin lesion task | | | | | | | | | |
| FedAvg | +17.58 | +7.41 | +0.66 | -2.86 | +7.41 | +2.51 | +9.87 | +6.27 | +1.33 |
| FedProx | +12.05 | +12.24 | +2.06 | +2.36 | +6.66 | +0.96 | +15.95 | +5.64 | +6.87 |
| FedDyn | +19.55 | +15.50 | -1.82 | +10.39 | +14.20 | +7.00 | +21.47 | +13.39 | +4.28 |
| SCAFFOLD | +0.72 | +4.01 | +3.45 | +1.28 | +9.05 | +6.93 | -1.67 | -3.94 | +7.45 |
| FedSAM | +4.50 | +7.51 | +1.39 | +17.18 | +16.82 | +5.57 | +14.41 | +7.72 | +2.88 |
| FedSpeed | +19.06 | +9.10 | +1.54 | +25.75 | +11.52 | +5.02 | +21.47 | +7.75 | +9.05 |
| FedSMOO | +19.87 | +11.11 | +3.16 | +2.28 | +12.53 | +2.27 | +34.51 | +7.39 | +5.32 |
| FedGamma | +8.40 | +4.00 | +4.67 | +7.66 | +7.03 | +5.18 | -0.69 | +1.51 | +6.91 |
| FedLESAM | +14.85 | +12.51 | +3.34 | +8.82 | +4.91 | -1.36 | +19.33 | +5.57 | +2.79 |
| FedWMSAM | +16.66 | +21.22 | +16.08 | +18.33 | +29.10 | +17.27 | -0.54 | -1.10 | +1.84 |
| Blood cell task | | | | | | | | | |
| FedAvg | +8.70 | +5.42 | -1.00 | +2.72 | +1.12 | -0.66 | +0.38 | +0.26 | -0.88 |
| FedProx | +13.42 | +3.44 | -1.67 | +11.16 | -2.35 | +2.95 | +0.12 | +0.28 | -0.50 |
| FedDyn | +7.32 | +5.07 | +0.32 | +28.01 | +9.25 | +4.84 | +0.58 | +0.06 | +0.14 |
| SCAFFOLD | +5.19 | +2.31 | +0.69 | +2.23 | -0.25 | -0.33 | +1.48 | +3.38 | +5.80 |
| FedSAM | +11.06 | -0.31 | -1.23 | +8.83 | -0.51 | +1.26 | +0.17 | +0.87 | -1.00 |
| FedSpeed | +23.67 | +4.64 | +0.08 | +19.88 | +3.52 | +1.56 | -0.06 | -0.15 | +0.30 |
| FedSMOO | +21.00 | +6.15 | +0.47 | +11.72 | +8.21 | +2.16 | +0.22 | -0.10 | +0.27 |
| FedGamma | +1.63 | -0.36 | +0.70 | -1.91 | -2.42 | -0.49 | +2.23 | -3.96 | +3.74 |
| FedLESAM | +6.11 | +2.79 | -0.48 | +18.00 | -0.18 | +1.75 | -0.21 | +0.64 | -0.52 |
| FedWMSAM | -1.78 | +15.51 | -5.82 | +17.64 | -8.17 | -5.26 | -1.47 | -2.92 | -12.50 |

Impact of Non-IID Data Distributions To analyze the impact of non-IID data distributions, we evaluate the proposed framework under three representative data skew types across multiple c values, as shown in Table 1. In detail, we analyze the performance differences at the respective stopping points between the proposed and validation-based early stopping approach. For the skin lesion task, the proposed approach achieves large average gains under severe heterogeneity ($c = 0.01/1$), reaching approximately +13.3%, +9.1%, and +13.4% for Dirichlet, Pathological, and quantity skew, respectively. As c increases to 1.0/3, the average gains decrease to around +3.5%, +5.1%, and +4.9%, indicating natural alignment with validation-based stopping as data distributions become IID.

For the blood cell task, similar trend is observed, where the proposed framework yields average gains of approximately +9.6%, +11.8%, and +0.3% under severe Dirichlet, Pathological, and quantity skew, respectively. Notably, across both tasks and skew types, the proposed approach achieves substantial gains under severe heterogeneity up to +34.5%/+28.0% (skin lesion/blood cell), which cannot be attributed to trivial decay of updates. This consistent pattern across tasks shows that the proposed criterion captures meaningful convergence under non-IID settings, rather than merely responding to diminishing updates. Thus, the proposed framework enables reliable hyperparameter tuning across diverse data distributions, with performance comparable to validation-based stopping.

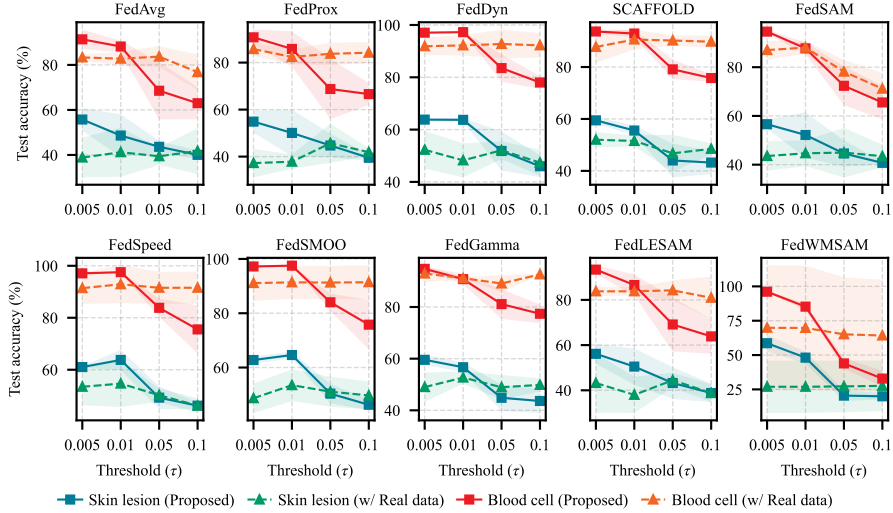


Fig. 4. Test accuracy (%) of FL methods evaluated under various threshold values with $\rho = 10$ for both validation-based and proposed early stopping. The solid curves denote the mean test accuracy, while the shaded regions indicate the standard deviation.

Impact of Threshold (τ) To investigate the effect of the stopping threshold τ on the proposed framework, we vary $\tau \in \{0.005, 0.01, 0.05, 0.1\}$ under *label skew* (Dirichlet) with $c = 0.1$. Note that for validation-based early stopping, we report the best test accuracy obtained at the same threshold using either validation loss or validation accuracy. As shown in Fig. 4, on the skin lesion task, the proposed framework shows a monotonic decrease in test accuracy as τ increases, with average reductions of approximately 18.4% across FL methods. In particular, FedDyn decreases from 63.8% and 63.7% at $\tau \in \{0.005, 0.01\}$ to 51.82% and 46.0% at $\tau \in \{0.05, 0.1\}$, while FedSMOO decreases from 64.6% to 46.3%. This trend indicates that large thresholds cause early termination, which enables rapid screening of configurations but limits performance.

A similar trend is observed on the blood cell task when compared with validation-based early stopping. At $\tau \in \{0.005, 0.01\}$, the proposed framework generally matches or exceeds the validation-based baseline across most FL methods, for example achieving 97.3% versus 92.2% for FedDyn and 97.5% versus 91.4% for FedSMOO. As τ increases to 0.05 and 0.1, the proposed accuracy drops markedly below the validation-based results, reaching 83.5% and 78.0% for FedDyn, and 84.0% and 75.8% for FedSMOO. This comparison shows that large thresholds enable fast evaluation but stop training too early to reach the optimum round. By contrast, small thresholds allow longer optimization, driving the model toward solutions closer to the optimal global model. Taken together, these results establish τ as a simple and effective control knob for balancing fast evaluation and convergence toward near-optimal models.

Table 2. Performance and stopping behavior of the proposed approach in terms of the stopping round (r^*) and corresponding test accuracy ($Acc.$), under $\tau = 0.1$ and $\rho = 10$. The $\Delta_{Acc.}$ and Δ_r denote the accuracy gain and round difference, respectively, relative to the best validation-based baseline at its stopping point.

| Method | Skin lesion task | | | | Blood cell task | | | |
|----------|------------------|-------|-----------------|------------|-----------------|-------|-----------------|------------|
| | Acc. (%) | r^* | $\Delta_{Acc.}$ | Δ_r | Acc. (%) | r^* | $\Delta_{Acc.}$ | Δ_r |
| FedAvg | 14.29 | 15.7 | - | +5.3 | 12.50 | 17.0 | - | +7.0 |
| FedProx | 14.29 | 16.7 | - | +6.7 | 12.50 | 14.0 | - | +4.0 |
| FedDyn | 14.29 | 20.0 | - | +10.0 | 12.50 | 20.7 | - | +10.7 |
| SCAFFOLD | 14.29 | 26.0 | - | +15.7 | 12.50 | 22.7 | - | +12.7 |
| FedSAM | 14.29 | 17.7 | - | +7.7 | 12.50 | 15.0 | - | +5.0 |
| FedSpeed | 14.29 | 19.7 | - | +9.7 | 12.50 | 19.7 | - | +9.7 |
| FedSMOO | 14.29 | 21.0 | - | +11.0 | 12.50 | 20.3 | - | +10.3 |
| FedGamma | 14.29 | 25.3 | - | +15.3 | 12.50 | 20.7 | - | +10.7 |
| FedLESAM | 14.29 | 13.3 | - | +3.3 | 12.50 | 15.3 | - | +5.3 |
| FedWMSAM | 14.29 | 21.0 | - | +10.7 | 12.50 | 22.0 | - | +9.7 |

Note. The symbol ‘-’ denotes no difference.

Ablation Study To validate the framework’s efficiency, we conduct an ablation study focused on handling bad configurations. In this scenario, the global model fails to learn, achieves only random-guess level accuracy 14.29%/12.50% (skin lesion/blood cell). As discussed in the threshold analysis, we use a large τ to enable fast evaluation and early termination. As shown in Table 2, the proposed framework requires only 3.3–15.7 additional rounds compared to the best validation-based baseline across all FL methods, far below the fixed budget of 500 rounds. On average, the proposed framework stops $\Delta_r \approx +9.5$ rounds later for the skin lesion task and $\Delta_r \approx +8.5$ rounds later for the blood cell task, relative to the best validation-based baseline. Note that this is less than 2% of the fixed-round budget, enabling rapid screening of bad configurations with minimal overhead. Therefore, the numerical results demonstrate that large τ enables efficient resource savings, particularly during early-stage tuning in FL.

4 Conclusion

In this work, we propose a data-free early stopping framework that identifies the stopping point via global task vector dynamics. The numerical results show that by tuning the threshold, our framework can either extend training for better performance or match the efficiency of validation-based baselines. Moreover, our framework significantly reduces the computational waste of fixed-round training by screening ineffective trials. The proposed approach stops comparably to validation-based approach, requiring only 9.5/8.5 (skin lesion/blood cell) additional rounds on average for FL methods. Thus, this work validates the feasibility of data-free early stopping, enabling resource-efficient tuning of FL methods.

Disclosure of Interests. The authors have no competing interests to declare relevant to this article’s content.

References

1. Acar, D.A.E., Zhao, Y., Matas, R., Mattina, M., Whatmough, P., Saligrama, V.: Federated learning based on dynamic regularization. In: Proc. ICLR. Vienna, Austria (May 2021)
2. Acevedo, A., Merino, A., Alférez, S., Molina, Á., Boldú, L., Rodellar, J.: A dataset of microscopic peripheral blood cell images for development of automatic recognition systems. *Data Br.* **30** (Apr 2020)
3. Antunes, R.S., André da Costa, C., Küderle, A., Yari, I.A., Eskofier, B.: Federated learning for healthcare: Systematic review and architecture proposal. *ACM Trans. Intell. Syst. Technol.* **13**(4), 1–23 (May 2022)
4. Bakas, S., Li, X., Shah, P., Roth, H.R.: Federated learning in healthcare: From research to real-world deployment. *Annu. Rev. Biomed. Eng.* **28** (Jan 2026)
5. Chen, C., Liao, T., Deng, X., Wu, Z., Huang, S., Zheng, Z.: Advances in robust federated learning: A survey with heterogeneity considerations. *IEEE Trans. Big Data* **11**(3), 1548–1567 (2025)
6. Dai, R., Yang, X., Sun, Y., Shen, L., Tian, X., Wang, M., Zhang, Y.: Fedgamma: Federated learning with global sharpness-aware minimization. *IEEE Trans. Neural Netw. Learn. Syst.* **35**(12), 17479–17492 (Dec 2024)
7. Fan, Z., Hu, S., Yao, J., Niu, G., Zhang, Y., Sugiyama, M., Wang, Y.: Locally estimated global perturbations are better than local perturbations for federated sharpness-aware minimization. In: Proc. ICML. Vienna, Austria (Jul 2024)
8. Foret, P., Kleiner, A., Mobahi, H., Neyshabur, B.: Sharpness-aware minimization for efficiently improving generalization. In: Proc. ICLR. Vienna, Austria (May 2021)
9. Ilharco, G., Ribeiro, M.T., Wortsman, M., Schmidt, L., Hajishirzi, H., Farhadi, A.: Editing models with task arithmetic. In: Proc. ICLR. Kigali, Rwanda (May 2023)
10. Joshi, M., Pal, A., Sankarasubbu, M.: Federated learning for healthcare domain-pipeline, applications and challenges. *ACM Trans. Comput. Healthc.* **3**(4), 1–36 (Nov 2022)
11. Kairouz, P., McMahan, H.: Advances and Open Problems in Federated Learning, *Found. Trends Mach. Learn.*, vol. 14. Now Publishers (2021)
12. Karimireddy, S.P., Kale, S., Mohri, M., Reddi, S., Stich, S., Suresh, A.T.: Scaffold: Stochastic controlled averaging for federated learning. In: Proc. ICML. Virtual Event (Jul 2020)
13. Khodak, M., Tu, R., Li, T., Li, L., Balcan, M.F.F., Smith, V., Talwalkar, A.: Federated hyperparameter tuning: Challenges, baselines, and connections to weight-sharing. In: Proc. NeurIPS. Virtual Event (Dec 2021)
14. Lee, Y., Gong, J., Choi, S., Kang, J.: Revisit the stability of vanilla federated learning under diverse conditions. In: Proc. MICCAI. Daejeon, Republic of Korea (Sep 2025)
15. Lee, Y., Lee, H., Gong, J., Cao, Y., Kang, J.: When to stop federated learning: Zero-shot generation of synthetic validation data with generative ai for early stopping. In: Proc. IEEE BigData. Macau, China (Dec 2025)
16. Lee, Y., Lee, H., Gong, J., Cao, Y., Kang, J.: Debunking optimization myths in federated learning for medical image classification. In: Proc. EMAI Workshop at MICCAI. Daejeon, Republic of Korea (Sep 2025)
17. Li, H., Zhang, Y., Zhang, S., Wang, M., Liu, S., Chen, P.Y.: When is task vector provably effective for model editing? a generalization analysis of nonlinear transformers. In: Proc. ICLR. Singapore (Apr 2025)

18. Li, M., Xu, P., Hu, J., Tang, Z., Yang, G.: From challenges and pitfalls to recommendations and opportunities: Implementing federated learning in healthcare. *Medical Image Analysis* **101** (Apr 2025)
19. Li, Q., Diao, Y., Chen, Q., He, B.: Federated learning on non-iid data silos: An experimental study. In: Proc. IEEE ICDE. Kuala Lumpur, Malaysia (May 2022)
20. Li, T., Sahu, A.K., Talwalkar, A., Smith, V.: Federated learning: Challenges, methods, and future directions. *IEEE Signal Process. Mag.* **37**(3), 50–60 (May 2020)
21. Li, T., Sahu, A.K., Zaheer, M., Sanjabi, M., Talwalkar, A., Smith, V.: Federated optimization in heterogeneous networks. In: Proc. MLSys. Austin, United States (Mar 2020)
22. Li, T., Huang, Y., Jiang, L., Liu, C., Xie, Q., Du, W., Wang, L., Wu, K.: Fedwmsam: Fast and flat federated learning method via weighted momentum and sharpness-aware minimization. In: Proc. NeurIPS. San Diego, United States (Dec 2025)
23. McMahan, B., Moore, E., Ramage, D., Hampson, S., y Arcas, B.A.: Communication-efficient learning of deep networks from decentralized data. In: Proc. AISTAT. Fort Lauderdale, United States (Apr 2017)
24. Niu, Z., Dong, H., Qin, A.K., Gu, T.: Flrce: Resource-efficient federated learning with early-stopping strategy. *IEEE Trans. Mob. Comput.* **23**(12), 14514–14529 (Dec 2024)
25. Peloquin, D., DiMaio, M., Bierer, B., Barnes, M.: Disruptive and avoidable: Gdpr challenges to secondary research uses of data. *Eur. J. Hum. Genet.* **28**(6), 697–705 (Mar 2020)
26. Qu, Z., Li, X., Duan, R., Liu, Y., Tang, B., Lu, Z.: Generalized federated learning via sharpness aware minimization. In: Proc. ICML. Baltimore, United States (Jul 2022)
27. Rajpurkar, P., Chen, E., Banerjee, O., Topol, E.J.: Ai in health and medicine. *Nat. Med.* **28**(1), 31–38 (Jan 2022)
28. Sun, Y., Shen, L., Chen, S., Ding, L., Tao, D.: Dynamic regularized sharpness aware minimization in federated learning: Approaching global consistency and smooth landscape. In: Proc. ICML. Hawaii, United States (June 2023)
29. Sun, Y., Shen, L., Huang, T., Ding, L., Tao, D.: Fedspeed: Larger local interval, less communication round, and higher generalization accuracy. In: Proc. ICLR. Kigali, Rwanda (May 2023)
30. Tschandl, P., Rosendahl, C., Kittler, H.: The ham10000 dataset, a large collection of multi-source dermatoscopic images of common pigmented skin lesions. *Sci. Data* **5**(1), 1–9 (Aug 2018)
31. Wang, H., Jin, Q., Li, S., Liu, S., Wang, M., Song, Z.: A comprehensive survey on deep active learning in medical image analysis. *Med. Image Anal.* **95** (Jul 2024)
32. Woo, S., Debnath, S., Hu, R., Chen, X., Liu, Z., Kweon, I.S., Xie, S.: Convnext v2: Co-designing and scaling convnets with masked autoencoders. In: Proc. IEEE/CVF CVPR. Vancouver, Canada (Jun 2023)
33. Xu, Y., Goodacre, R.: On splitting training and validation set: a comparative study of cross-validation, bootstrap and systematic sampling for estimating the generalization performance of supervised learning. *J. Anal. Test.* **2**(3), 249–262 (Oct 2018)
34. Yang, J., Shi, R., Wei, D., Liu, Z., Zhao, L., Ke, B., Pfister, H., Ni, B.: Medmnist v2-a large-scale lightweight benchmark for 2d and 3d biomedical image classification. *Sci. Data* **10**(1), 41 (Jan 2023)
35. Yao, Y., Rosasco, L., Caponnetto, A.: On early stopping in gradient descent learning. *Constr. Approx.* **26**(2), 289–315 (Apr 2007)